BeBeC-2016-D15

AN EFFICIENT METHODOLOGY FOR COMPREHENSIVE EVALUATION OF TURBOMACHINERY SOURCE MAPS

Bence Tóth and János Vad

Department of Fluid Mechanics,
Faculty of Mechanical Engineering,
Budapest University of Technology and Economics,
Bertalan Lajos u. 4-6, 1111, Budapest, Hungary

ABSTRACT

In order to establish guidelines for reducing the noise emitted by an axial flow fan, the case study-specific dominant noise sources are to be characterized. Beamforming based on a Phased Array Microphone (PAM) system offers a powerful diagnostics tool for such purpose. In general, the evaluation of the beamforming maps involves certain subjective and arbitrary elements. This paper presents an objective, mathematically algorithmized methodology for concerted evaluation of beamforming maps extending over a broad frequency band, in order to quantify and to localize the dominant blade passage-periodic rotating broadband noise sources. The methodology is illustrated in a case study. The circumferential source strength distribution is transformed into the spatial frequency domain in each third-octave band, with use of Fourier analysis. Using these spectra, significant noise peaks are identified on the basis of a natural criterion. The peaks are assigned to physically distinct noise sources using a fuzzy c-means clustering algorithm. The underlying physical mechanisms of the resulting clusters, i.e. the coupled aerodynamic-aeroacoustic causes of the related noise, are to be analysed using literature data and detailed computational simulations.

NOMENCLATURE

Abbreviations

FCM	Fuzzy c-Means
FFTW	Fast Fourier Transform in the West
PAM	Phased Array Microphone
PSF	Point Spread Function
RMS	Root Mean Square
ROSI	Rotating Source Identifier

Latin letters

A	Pa	mode amplitude
a	-	dimensionless mode amplitude
B	-	blade number
c	-	number of fuzzy clusters
D	m	diameter of aperture
f	Hz	third-octave band mid-frequency
i	-	running index
j	-	running index
k	-	number of clusters
l	Pa	limit of significant noise source strength
L	dB	source strength level
n	1/rad	spatial frequency
m	-	fuzzifier
N	-	number of data points
P	Pa	source strength
p	-	dimensionless source strength
S	-	set of data points
x	-	data element to be clustered
w	-	membership function

Indices

B	maximum value in the beamforming maps
f	third-octave band mid-frequency
OPT	optical
t	tip

Greek letters

β	rad	mode phase angle
λ	m	wavelength
ϕ	-	dimensionless spatial frequency
φ	rad	circumferential angle
κ	-	resolution limit multiplier
μ	-	cluster centre
Θ	rad	least angle between two separated sources

1 INTRODUCTION AND OBJECTIVES

Regulations are becoming more and more stringent about the noise emitted by turbomachinery. Fans are important in particular, because they operate in large numbers and in close vicinity of humans, therefore their environmental impact is considerable. Reducing the noise of axial fans through redesigning the fan elements emitting the most intense noise is an important aim. The tonal fan noise, e.g. being due to rotor-stator interaction, is successfully suppressed by appropriate blade geometrical modifications such as blade skew [1], and is out of the scope of this paper. A significant trend is to control rotating *broadband* noise sources – e.g. blade tip leakage flow [2] –, being in the focus of the present paper.

In order to obtain guidelines for redesigning the fan for reducing the broadband noise, an essential preliminary step is to *quantify* and to *localize* the dominant noise sources, being specific to the fan under investigation. A *noise source* is defined herein as a coupled aerodynamic-aeroacoustic phenomenon that is physically distinct, i.e. that is physically separable from other phenomena in the flow region under investigation. For example, near the blade tip radius, the tip leakage flow is found as a noise source, since it is viewed as a flow phenomenon being physically distinct from other flow phenomena in the near-tip region, such as casing boundary layer, blade boundary layers, and core flow in the blade passage. In general, a broadband noise source is distributed both *spectrally* – i.e. over a broader sound frequency band – and *spatially*. Since the Phased Array Microphone (PAM) technique, supported by a suitable beamforming algorithm, provides both *spectrally* and *spatially* resolved information, it represents a powerful tool for characterizing the dominant broadband noise sources.

It is to be noted that the beamforming results are usually evaluated with involvement of certain subjective factors and arbitrarily established criteria, as discussed below.

a) The generation of aeroacoustic images usually involves "cut-and-try" approaches, necessitating human intervention, e.g. in setting the proper dynamic range for spectacular representation of the imaged noise sources.

b) The visual manner of evaluation is a subjective approach. For example, in reference [3], the proper separation of pairs of spots of noise intensity maxima, i.e. the representation of spatial resolution, is judged by observing the beamforming maps visually. The details of the source maps obtained for low-speed axial fan rotors in [4-6] are evaluated in an intuitive manner, on the basis of visual inspection.

c) A further factor of subjectivity is the application of optics-based, arbitrarily chosen criteria for judging the spatial resolving power of the beamforming technique. Resolution criteria established for *human vision* are dubious to be applied as resolution criteria in acoustics. Examples for optics-based criteria for spatial resolution are the Rayleigh limit, the Dawes limit, and the Sparrow limit [7]. These criteria are based mathematically on the point spread functions (PSF), and were historically introduced as subjective criteria depending on the resolving power of the eye of the observer. They are given in the following form, where only the multiplier κ varies between the various criteria:

$$\sin\Theta \approx \kappa \frac{\lambda}{D_{OPT}} \qquad (1)$$

In this equation, D_{OPT} is the diameter of the optical aperture [m], λ is the wavelength [m] and Θ [rad] is the smallest viewing angle at which two sources can be separated.

As noted before, these formulae originate from optical background. When an infinitely distant point source emits light that is observed through a circular aperture, an image is formed consisting of fringes: lighter and darker regions. This is termed the PSF. When two identical sources are present, different image patterns form, depending on the separation between the sources. Between the two largest intensity peaks of the PSF, a "dip", i.e. intensity decrease, occurs. Such dip is expressed as the percentage of the peak intensity. The Rayleigh, Dawes and Sparrow limits define the resolving power based on the magnitude of the dip.

In evaluation of phased array microphone results, the use of the Rayleigh limit [3, 6, 8] and the Sparrow limit [3] is apparent. Table 1, based on data in reference [7], presents how κ and the dip vary for the various optics-based limits. These data demonstrate how the spatial resolution (correlating with κ), as well as the detectability of two distinct sources (correlating with the dip), are exposed to subjectivity if they are specified by means of optics-based criteria of arbitrary choice.

Table 1. κ multipliers and dip magnitudes for various optical resolution criteria

Limit type	κ	*dip*
Rayleigh	1.22	26.5%
Dawes	1.03	5%
Sparrow	0.96	0%

d) Besides subjectivity, the reliability of arbitrary application of optics-based criteria in judging the spatial resolution of fan aeroacoustic images (utilizing a presumed wave optical – wave acoustic analogy) is also limited by the following facts (conf. [9]).

- The optics-based criteria refer to the separation of two point sources of identical strength. This is rarely fulfilled when analysing beamforming maps for fan rotors. For example, the studies documented in [6] especially aimed at discovering the spanwise non-uniform intensity distribution of rotor noise sources.
- The imaging device is required to have a circular aperture for the optics-based criteria. Contrarily, e.g. in [6], the microphones of the array are arranged along a logarithmic spiral curve.
- For the optics-based criteria, relying on the Fraunhofer diffraction, the observer is presumed to be located infinitely far from the source. This implies that the incoming waves reaching the imaging device can be assumed as planar waves. Contrarily, in fan noise imaging, the distance between the fan and the array is often confined to the order of magnitude of some times the rotor tip diameter. For example, in [6], the array was installed at a distance of ≈ 2 tip diameter from the fan inlet.

The aim of the methodology presented herein is the objective quantification and localization of dominant, blade passage-periodic, and physically distinct broadband noise sources in axial fan rotors. Objectivity is achieved by a mathematically established, algorithmic data processing and evaluation procedure, being free from any subjective factors and arbitrarily established criteria discussed above. The main features of the methodology, in relationship with the applied Fourier and cluster analyses outlined later, are as follows.

- *Quantification and localization.* Both the Fourier amplitude spectrum and phase spectrum of the beamforming data sets are exploited, for quantifying as well as localizing the noise sources.
- *Dominance.* The Fourier amplitude spectrum provides a tool for identifying the dominant (most significant) components of noise.
- *Blade passage-periodicity.* Noise sources being characteristic periodically for each rotor blade passage are of present interest. The Fourier amplitude spectrum provides a tool for

spatial filtration of the beamforming data, eliminating the perturbations superimposed on blade passage-periodic effects.

- *Broadband noise sources.* The Fourier spectra are evaluated over all third-octave frequency bands under interrogation in a concerted manner. By such means, spatially distributed broadband noise sources associated with physically distinguishable flow phenomena are identified. The noise sources, being distributed both spectrally and spatially, are identified by means of a cluster analysis.

Preliminary studies to this methodology are presented in [10]. The application of the methodology is presented through a case study of an axial flow ventilation fan, the upstream-radiated noise of which has been subjected to PAM investigation.

2 CASE STUDY

The investigated fan is an axial flow industrial cooling fan. Its properties as well as the instrumentation, data acquisition and processing are thoroughly reported in [6], also providing further references about the details. Only the most representative data are summarized herein. The rotor has B=5 blades, tip diameter of 0.30 m and a hub-to-tip diameter ratio of 0.3. It has a rotor-only one-stage configuration. The angular frequency of the rotor is 149.75 rad/s measured via an optical transducer. The signal of the optical transducer also provided a means for identifying the angular position of the rotor, being necessary for the Rotating Source Identifier (ROSI) [11] algorithm applied. The noise radiated upstream of the fan has been recorder by the PAM system, centred on the axis of rotation.

The noise was recorded using an OptiNav, Inc. Array 24 PAM system, and the accompanying processing equipment, i.e. amplifier and analogue-to-digital converter. This system has 24 microphones arranged in logarithmic spirals in order to suppress sidelobes. The array was placed perpendicularly to the axis of rotation of the fan on the suction side at 0.5 m distance from the inlet. Sampling frequency was set to 44.1 kHz, and the duration of the acquired data was 20 s.

The acquired data was processed using an in-house implementation of the ROSI algorithm. ROSI works by calculating the time delays between each microphone and each point of the rotating beamform grid, re-interpolating the recorded pressure signals, thus removing the Doppler shift from the results, and placing the rotating target into a stationary coordinate system with respect to the PAM. A sample length of 1024 was used for the Fourier transformation incorporated in the PAM data processing, and the diagonal elements of the cross-spectral matrices were set to zero in order to remove the effects of uncorrelated noise. After beamforming, narrow-band maps were constructed. By summing the appropriate maps, third-octave band beamforming maps were created centred on 2000 Hz, 2500 Hz, 3150 Hz, 4000 Hz, 5000 Hz and 6300 Hz.

Figure 1 shows the maxima of the beamforming maps obtained by ROSI in each frequency bin. It demonstrates the dominance of broadband noise, the sources of which are in the focus of the discussion presented herein.

Figure 2 presents an example for the beamforming maps, related to the third-octave band centred on 6300 Hz. The basic periodicity originating from the blades is clearly apparent. However, there appear some rotational asymmetries in the noisiest region near the tip radius. Furthermore, it is uncertain whether the local peaks being in between the absolute maxima are to be considered as “significant” peaks manifesting the presence of distinct noise sources, or are to be neglected in further discussion.

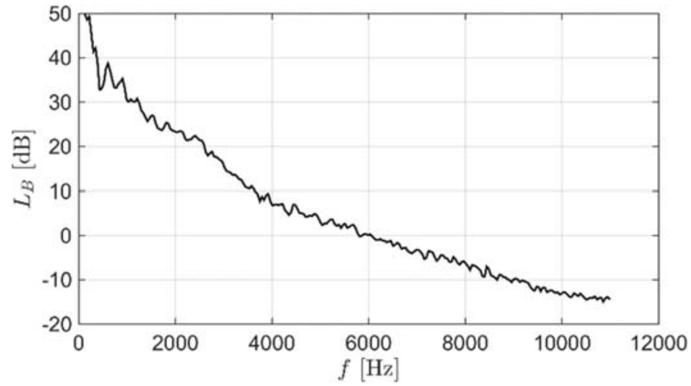

Fig. 1. Fan noise spectrum, reproduced from [6]

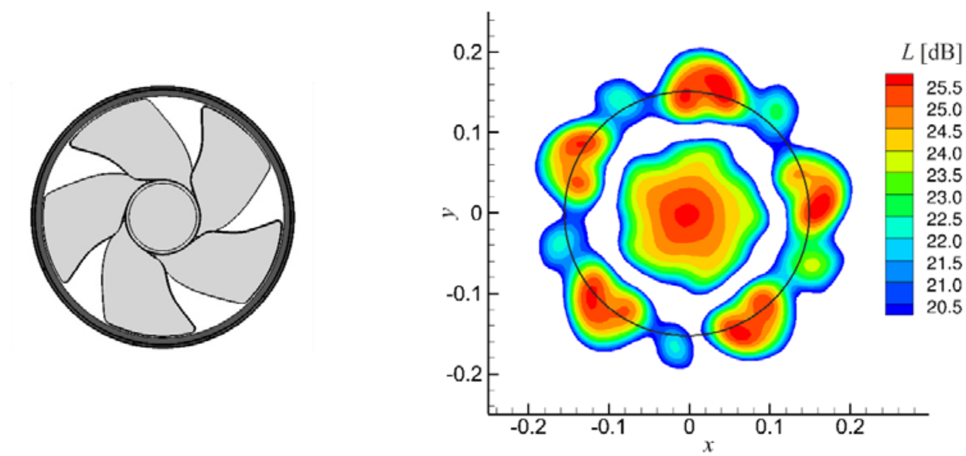

Fig. 2. Sketch of the fan, and beamforming map at 6300 Hz (based on [6]). The circle in the map indicates the fan casing.

On the left-hand side of Figure 2, an illustrative sketch of the fan is presented. The right-hand side of the figure presents an example for the beamforming maps, related to the third-octave band centred on 6300 Hz. It is noted that, at the present level of discussion, the view of the fan and the beamforming map in Fig. 2 are not in correspondence from the viewpoint of angular position of the rotor. The basic periodicity originating from the blades is clearly apparent. However, there appear some rotational asymmetries in the noisiest region near the tip radius. Furthermore, it is uncertain whether the local peaks being in between the absolute maxima are to be considered as "significant" peaks manifesting the presence of distinct noise sources, or are to be neglected in further discussion.

3 SPATIAL FOURIER TRANSFORM

In this analysis, the dominant noise sources related to the *individual blades* are to be discovered. This is necessitated by the aim of establishing guidelines for aerodynamic-aeroacoustic redesign of the blades, and their environment. Therefore the noise sources are expected to have a periodicity related to the number of the blades, or an integer multiplier of them. A significant average (non-periodic) noise is also expected to be present, because of background noise as well as measurement and processing uncertainties. Any other periodicity is regarded as an effect of some kind of perturbation, e.g. non-uniform upstream flow conditions, or interaction noise resulting from the presence of struts. Further discussion on various types of perturbations is given in [10].

The PAM-measured noise detected at the blade tip diameter of the fan has been chosen herein as a spectacular case study, illustrating the capabilities of the presented methodology. One reason is that the fan exhibits significant noise in the near-tip region (as previous investigations, e.g. in [6], demonstrate). Furthermore, e.g. the beamforming map in Fig. 2 suggests that the near-tip region provokes the co-existence of multiple noise sources, deserving a more detailed systematic analysis. In order to quantify the information on the noise emission, for each third-octave band of centre frequency f, the calculated source strength, P_f, is extracted from the beamforming maps along a circumferential path parametrised by φ around the fan at the tip diameter. The source strength functions along the circumference are shown in Fig. 3. The source strength is normalised by a reference value for the analysed frequency bands.

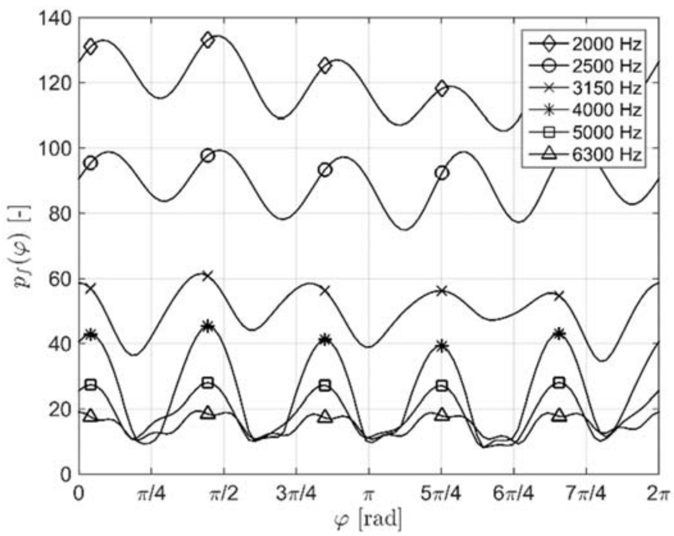

Fig. 3. The distribution of dimensionless source strength along the circumference of the rotor

In order to obtain information about the aforementioned periodic components, the spatial Fourier transform of the signals in Fig. 3 was computed using 100 samples. This sample size was chosen because it is in agreement with the grid resolution of the original beamforming maps, it allows for the calculation of the exact amplitudes of the fivefold and tenfold periodic components, and it is a product of small primes, enabling a rapid calculation using the Fast Fourier Transform in the West (FFTW) algorithm [12]. The source strength distribution is then decomposed as described by Eq. (2).

$$P_f(\varphi) = \sum_{n=0} A_f(n) \cos\left(n\left(\varphi - \beta_f(n)\right)\right) \tag{2}$$

Here m is the spatial frequency, A_f is the amplitude and β_f is the phase shift, the location of the first maximum of the cosine. For easier understanding, the spatial frequency was normalized by the blade count B, thus the dimensionless spatial frequency ϕ is a direct measure of how many periods the chosen harmonic component contains per blade passage.

$$\phi = n / B \tag{3}$$

The amplitudes were normalized by a reference value, thus the dimensionless amplitudes a_f were obtained.

An obtained dimensionless amplitude spectrum is shown in Fig. 4 as an example. The presence of a large mean value can clearly be seen at ϕ=0 (average, i.e. the component associated with zero spatial frequency), accompanied by outstanding peaks at ϕ=1 and ϕ=3. Some additional variation in amplitude can be seen at other values of ϕ as well. Naturally arises the question, which peak is to be considered important and analysed further on. Based on the expected periodicity, a threshold can be defined as the largest perturbation amplitude, i.e. the maximum of the amplitudes whose spatial frequency is not at an integer multiplier of the blade number. In terms of dimensionless spatial frequency, it means that it is not an integer value. Examples for perturbations of such kind are as follows [10]: non-uniform tip clearance along the circumference, or variation of blade geometry. The amplitude threshold for a peak to be characterized as significant is chosen as the maximum perturbation amplitude:

$$l_f = \max A_f(\phi) \quad \text{where} \quad \phi = \frac{1}{B}, \frac{2}{B} \ldots \frac{B-1}{B} \tag{4}$$

This threshold is calculated and applied for each investigated third-octave band represented by the subscript *f*. Only those peaks are retained as "significant" peaks for further processing, the amplitude of which is larger than the corresponding threshold value.

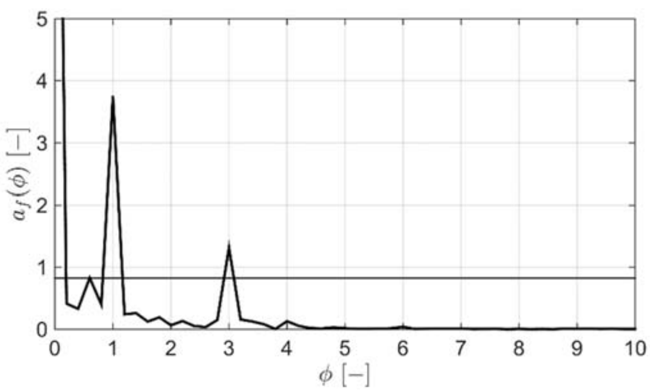

Fig. 4. Dimensionless spatial frequency spectrum of the third-octave band centred on 6300 Hz

In Figure 4, this threshold is shown by the horizontal straight line. Based on this criterion, e.g. in the 6300 Hz band, only the peaks at ϕ=0, 1 and 3 are kept for further processing.

Using the phase information obtained from the Fourier transform, the angular location of the component peaks can also be determined. This is shown in Fig 5 for which the horizontal axis shows the centre frequency of the band, and the vertical one shows the normalised angle inside the blade passage (the 0÷1 range covers the entire blade passage). Here, all significant peaks are shown. For example, for the 6300 Hz band, the single ϕ=1 peak is shown together with all three ϕ=3 peaks, thus indicating all significant local maxima of the beamforming map.

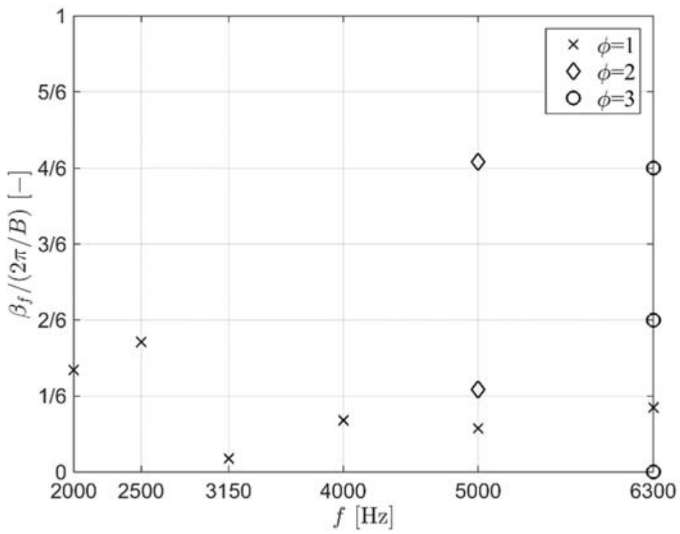

Fig. 5. The important source peaks as a function of frequency and angular position

4 CLUSTERING

After the significant source peaks have been identified, they are to be analysed, grouped ("clustering"), and assigned to distinct source mechanisms. In the current analysis, broadband noise sources are considered, because the emitted noise spectrum of the fan is characteristically broadband. The following considerations are made. a) A source mechanism is expected to be connected to a specific location of the geometry, i.e. it is to be localised at a characteristic position inside the blade passage. b) A broadband source is expected to emit noise in consecutive third-octave frequency bands. Based on a) and b), the [frequency-angular position] plane presented in Fig. 5 offers a suitable scene for clustering the significant source peaks presented over the plane.

The next aim is to classify these peaks in an objective way. To create groups of similar elements, clustering is often used. It is a quickly developing field, originally used in life sciences [13, 14], but nowadays more-and-more applied in computerised data analysis [15, 16].

The aim of the method is to create clusters that contain the elements of the original data set consisting of N points, in a way that the elements in one cluster are more similar to each other in some way, than to elements of other clusters. The simplest method is called *k-means clustering* [17] that aims to find a predefined k number of clusters, where the measure of similarity between two points is a norm of their difference, usually the Euclidean norm. Given a set S consisting of individual observations x_i, the task is finding the subsets S_j and their means of points μ_j that minimise the following expression:

$$\arg\min_{S} \sum_{i=1}^{N} \sum_{j=1}^{k} \left\| x_i - \mu_j \right\|^2 \qquad (5)$$

In the current case, the aim is to create clusters of sources that are close to each other in space (*localised*) and emit noise in neighbouring third-octave bands (*broadband*). From the current point of view, a broadband source means not only that a given source emits noise in consecutive third-octave bands but also that the noise within a certain third-octave band might be the result of *neighbouring* source mechanisms, having an overlapping spectrum in the frequency band under consideration. Therefore the clustering algorithm has to be able to assign any given peak to more neighbouring clusters.

In order to achieve that, fuzzy clustering is used. Here a $w_{i,j}$ membership function is defined that may take values in the interval [0, 1]. Its value indicates how much a certain element x_i belongs into the cluster S_j. That way, fuzzy clustering allows a peak to be part of two (or more) source mechanisms. The algorithm called *fuzzy c-means* (FCM) clustering [17] is used in the present investigation. FCM is similar to k-means clustering given that it arranges data points into clusters to minimize the distances between each element of the same cluster, but it includes the membership function to allow the clusters to overlap. The problem is to minimise the expression in (6).

$$\arg\min_{S} \sum_{i=1}^{N} \sum_{j=1}^{c} w_{i,j}{}^{m} \left\| x_i - \mu_j \right\|^2 \tag{6}$$

Here the centre of the *j*-th cluster is given as:

$$\mu_j = \frac{\sum_{i=1}^{N} w_{i,j}{}^{m} x_i}{\sum_{i=1}^{N} w_{i,j}{}^{m}} \tag{7}$$

The algorithm requires the number of clusters to be predefined, similarly to k-means clustering. For an objective definition of the reasonable number of clusters, *c*, the following considerations were made. a) The *upper limit* of the reasonable number of clusters is tailored by the fact that broadband noise sources are to be discovered. This means that the sought clusters should extend over *at least two consecutive frequency bands*. a) The *lower limit* of the reasonable number of clusters is tailored by the fact that the grade of membership should not fall below a certain limit, i.e. ≈ 0.5, for any peak. This implies that each peak is assigned firmly either to a certain noise source, or simultaneously to two neighbouring sources of overlapping spectrum.

The expressions (6) to (7) contain a parameter *m,* called fuzzifier, which is used to set how fuzzy the sets may be. Its value is chosen as 2, as usual in absence of previous knowledge [18].

The fuzzy c-means clustering method has formerly been used to analyse geophysical [19], medical (MRI) [20] and chemical [21] data. To the authors' best knowledge, this paper presents its first application to identification of rotating noise sources in turbomachinery. For data processing, a freely available toolkit was used [22, 23].

Figure 6 presents the results of the FCM clustering. The reasonable number of clusters, *c*=3 has been established by iterative use of the FCM toolkit, and considering the upper and lower limiting criteria a) and b) outlined above. The resultant clusters are well-separated, with significant gaps between them. The bottom-left cluster contains the lowest frequency sources, from 2000 Hz to 3150 Hz in its core. The bottom-right one contains 5000 Hz and 6300 Hz peaks on the lower side of the blade passage, while the top-right cluster contains just two peaks of high frequency: one at 5000 Hz and one at 6300 Hz. The 4000 Hz peak is in between the bottom-left and bottom-right cluster, having approximately equal grades of membership with respect to both clusters. In the present case, it suggests that the 4000 Hz peak is a result of two separate source mechanisms the broadband spectra of which overlap in the third-octave band centred on 4000 Hz.

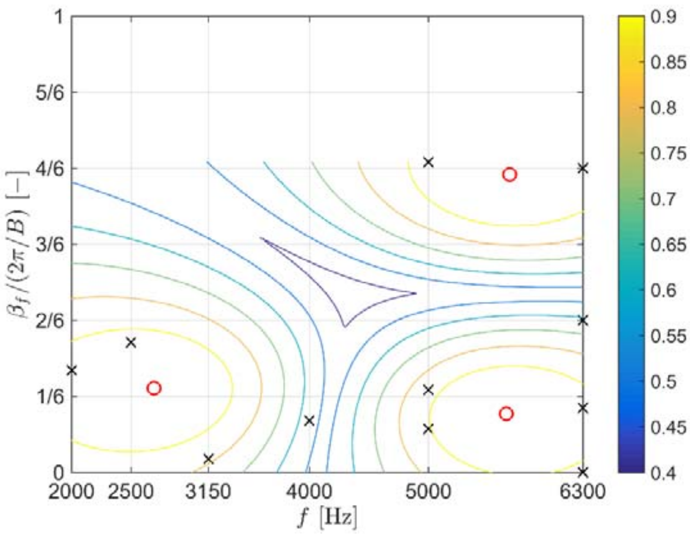

Fig. 6. Results of clustering. x *– peak locations,* o *– , lines: membership iso-lines*

5 SUMMARY AND FUTURE REMARKS

A novel method has been presented, providing a tool for quantification and localization of dominant, blade passage-periodic, and physically distinct rotating broadband noise sources in axial flow turbomachinery, the noise of which is recorded by a PAM equipment centred on the axis of rotation. The method helps the discovery of dominant turbomachinery source maps in a completely objective and algorithmic manner, without any *a priori* knowledge on the details of blade geometry and blade aerodynamics. It can identify those peaks with the help of the Fourier transformation that are connected to the periodically repeated rotor blade passages. Thus, it is possible to make a classification of rotor-related, case study-specific noise sources. It provides a means to select the peaks of source strength to be judged significant in further processing. By introducing a definition of broadband noise source, it is able to determine clusters and group the identified significant peaks into them, using the FCM method.

In the case study example presented herein, it has objectively been pointed out that the near-tip rotor noise is dominated by three distinct noise sources. The identification of these three sources necessitated no *a priori* knowledge on blade geometry and blade aerodynamics. The following steps of research are as follows. a) The angular position of the blading is to be assigned to the clustering map in Fig. 6. b) On this basis, the three noise sources are to be localized relative to the blading. c) The noise sources are to be quantified with use of the appropriate components of the Fourier amplitude spectra. d) The PAM results are to be supplemented with literature survey, and aerodynamic experiments + simulations for quantitatively discovering the *underlying physics* (noise source mechanisms) of the three quantified and localized noise sources. e) By such means, guidelines can be formulated for moderation of fan noise related to these three noise sources.

ACKNOWLEDGEMENT

This work has been supported by the Hungarian National Fund for Science and Research under contract No. OTKA K 112277. The work relates to the scientific programs "Development of quality-oriented and harmonized R+D+I strategy and the functional model at BME" (Project

ID: TÁMOP-4.2.1/B-09/1/KMR-2010-0002) and "Talent care and cultivation in the scientific workshops of BME" (Project ID: TÁMOP-4.2.2/B-10/1-2010-0009).

REFERENCES

[1] T. Carolus. "Ventilatoren". Teubner Verlag, Viesbaden, 2003.

[2] S. Bianchi, A. Corsini, F. Rispoli and A. G. Sheard. "Far-Field Radiation of Tip Aerodynamic Sound Sources in Axial Fans Fitted with Passive Noise Control Features." ASME Journal of Vibration and Acoustics, 133, 051001-1:051001:11, 2011.

[3] R. P. Dougherty, R. C. Ramachandran and G. Raman. "Deconvolution of sources in aeroacoustic images from phased microphone arrays using linear programming." International Journal of Aeroacoustics, 12, 7 & 8, 699-718, 2013.

[4] O. Minck, N. Binder, O. Cherrier, L. Lamotte and V. Budinger. "Fan noise analysis using a microphone array." Proceedings of International Conference on Fan Noise, Technology and Numerical Methods (FAN2012), Senlis, France, 2012. ISBN 978-0-9572374-1-4.

[5] G. Herold and E. Sarradj. "Microphone array method for the characterization of rotating sound sources in axial fans." Proceedings of the International Conference on Fan Noise, Technology and Numerical Methods (FAN2015), Lyon, France, 2015. ISBN 978-0-9572374-3-8.

[6] T. Benedek and J. Vad, J. "Study on the effect of inlet geometry on the noise of an axial fan, with involvement of the phased array microphone technique." *ASME Paper* GT2016-57772 (accepted), 2016.

[7] T. S. McKechnie. "General theory of light propagation and imaging through the atmosphere." Springer, Cham – Heidelberg – New York – Dordrecht – London, 2016.

[8] J. Hald. "Combined NAH and beamforming using the same array." Brüel & Kjær Technical Note (2005-1), 2005.

[9] F. A. Jenkins and H. E. White. "Fundamentals of optics." Fourth edition. McGraw-Hill Primis Custom Publishing, New York, 1976.

[10] B. Tóth and J. Vad, J. "Fourier analysis of beamforming data at the tip of an axial fan rotor." Periodica Polytechnica, Mechanical Engineering. Paper ID 8935 (submitted), 2016.

[11] P. Sijtsma, S. Oerlemans and H. Holthusen. "Location of rotating sources by phased array measurements." Proceedings of the 7th AIAA/CEAS Aeroacoustics Conference, Maastricht, 2001. doi:10.2514/6.2001-2167

[12] M. Frigo and S. G. Johnson. "FFTW: An adaptive software architecture for the FFT." Proceedings of the 1998 IEEE International Conference on Acoustics, Speech and Signal Processing, 12, 1381-1384, 1998.

[13] K. Bailey. "Numerical Taxonomy and Cluster Analysis. Typologies and Taxonomies." Sage University Paper series on Quantitative Applications in the Social Sciences, 07-102. Thousand Oaks, CA: Sage, 1994. ISBN 9780803952591.

[14] R. C. Tryon. "Cluster Analysis: Correlation Profile and Orthometric (factor) Analysis for the Isolation of Unities in Mind and Personality." Edwards Brothers, Ann Arbor, Michigan, 1939.

[15] F. Can and E. A. Ozkarahan. “Concepts and effectiveness of the cover-coefficient-based clustering methodology for text databases.” ACM Transactions on Database Systems, 15, 4, 1990. doi:10.1145/99935.99938.

[16] M. Ester, H-P. Kriegel, J. Sander and X. Xu. “A density-based algorithm for discovering clusters in large spatial databases with noise.” In E. Simoudis, J. Han and U. M. Fayyad. Proceedings of the Second International Conference on Knowledge Discovery and Data Mining (KDD-96), AAAI Press, 226–231, 1996. ISBN 1-57735-004-9.

[17] B. Bede. “Mathematics of Fuzzy Sets and Fuzzy Logic.” Springer, Berlin Heidelberg, 2013. doi:10.1007/978-3-642-35221-8

[18] N. R. Pal and J. C. Bezdek. “On Cluster Validity for the Fuzzy c-Means Model.” IEEE Transactions on Fuzzy Systems, 3, 3, 1995.

[19] J. C. Bezdek, R. Ehrlich and W. Full. “FCM: The fuzzy c-means clustering algorithm.” Computers & Geosciences 10, 2, 191-203, 1984.

[20] M. N. Ahmed, S. M. Yamany, N. Mohamed, A. A. Farag and T. Moriarty, T. “A Modified Fuzzy C-Means Algorithm for Bias Field Estimation and Segmentation of MRI Data.” IEEE Transactions on Medical Imaging, 21, 3, 193–199, 2002.

[21] G. Barkó, J. Abonyi and J. Hlavay, J. “Application of fuzzy clustering and piezoelectric chemical sensor array for investigation on organic compounds.” Analytica Chimica Acta, 398, 2, 219-226, 1999.

[22] B. Balasko, J. Abonyi and B. Feil. “Fuzzy clustering and data analysis toolbox.” Department of Process Engineering, University of Veszprem, Veszprem, 2005. URL http://www.abonyilab.com/software-and-data/fclusttoolbox

[23] T. Kenesei, B. Balasko and J. Abonyi. “A MATLAB Toolbox and its Web based Variant for Fuzzy Cluster Analysis.” 7th International Symposium of Hungarian Researchers on Computational Intelligence. Budapest, 2006.